Correction

NEUROSCIENCE

Correction for "Single-nucleus RNA sequencing of mouse auditory cortex reveals critical period triggers and brakes," by Brian T. Kalish, Tania R. Barkat, Erin E. Diel, Elizabeth J. Zhang, Michael E. Greenberg, and Takao K. Hensch, which was first published May 13, 2020; 10.1073/pnas.1920433117 (*Proc. Natl. Acad. Sci. U.S.A.* **117**, 11744–11752).

The authors note that the following statement should be included at the end of the legend for Fig. 3: "Some of the data used in *B*, *C*, and *D* are readapted from the C57 dataset used in ref. 9." The authors also note that the following statement should be included at the end of the *Materials and Methods* section, on page 11751: "C57 data were readapted from ref. 9 in accordance with the Institutional Animal Care and Use Committee guidelines to reduce unnecessary use of animals. Statistics were taken internal to each genotype." The authors apologize for the oversight in not clearly identifying the dataset from their prior publication.

First published August 3, 2020.

www.pnas.org/cgi/doi/10.1073/pnas.2014145117

Single-nucleus RNA sequencing of mouse auditory cortex reveals critical period triggers and brakes

Brian T. Kalish[a,b,1], Tania R. Barkat[c,d,1,2], Erin E. Diel[c,d,1], Elizabeth J. Zhang[d], Michael E. Greenberg[a,3], and Takao K. Hensch[c,d,e,f,3]

[a]Department of Neurobiology, Harvard Medical School, Boston, MA 02115; [b]Division of Newborn Medicine, Department of Medicine, Boston Children's Hospital, Boston, MA 02115; [c]Department of Molecular and Cellular Biology, Harvard University, Cambridge, MA 02138; [d]Center for Brain Science, Harvard University, Cambridge, MA 02138; [e]F. M. Kirby Neurobiology Center, Department of Neurology, Boston Children's Hospital, Harvard Medical School, Boston, MA 02115; and [f]Child Brain Development, Canadian Institute for Advanced Research, Toronto, ON M5G 1M1, Canada

Contributed by Michael E. Greenberg, March 2, 2020 (sent for review November 27, 2019; reviewed by David F. Clayton and Étienne de Villers-Sidani)

Auditory experience drives neural circuit refinement during windows of heightened brain plasticity, but little is known about the genetic regulation of this developmental process. The primary auditory cortex (A1) of mice exhibits a critical period for thalamocortical connectivity between postnatal days P12 and P15, during which tone exposure alters the tonotopic topography of A1. We hypothesized that a coordinated, multicellular transcriptional program governs this window for patterning of the auditory cortex. To generate a robust multicellular map of gene expression, we performed droplet-based, single-nucleus RNA sequencing (snRNA-seq) of A1 across three developmental time points (P10, P15, and P20) spanning the tonotopic critical period. We also tone-reared mice (7 kHz pips) during the 3-d critical period and collected A1 at P15 and P20. We identified and profiled both neuronal (glutamatergic and GABAergic) and nonneuronal (oligodendrocytes, microglia, astrocytes, and endothelial) cell types. By comparing normal- and tone-reared mice, we found hundreds of genes across cell types showing altered expression as a result of sensory manipulation during the critical period. Functional voltage-sensitive dye imaging confirmed GABA circuit function determines critical period onset, while Nogo receptor signaling is required for its closure. We further uncovered previously unknown effects of developmental tone exposure on trajectories of gene expression in interneurons, as well as candidate genes that might execute tonotopic plasticity. Our single-nucleus transcriptomic resource of developing auditory cortex is thus a powerful discovery platform with which to identify mediators of tonotopic plasticity.

auditory cortex | GAD65 | Nogo receptor | single-cell sequencing

Activity-dependent plasticity shapes neural circuits in response to sensory experience during distinct developmental windows, termed "critical periods." Heightened plasticity at these times refines the anatomic and functional architecture across brain regions (1). Decades of work in the primary visual cortex (V1) have defined how activity drives molecular and cellular events to open and close critical periods (2–4). Far less detail is known in other sensory systems, such as the primary auditory cortex (A1), where biased early-life acoustic exposures lead to robust alterations in the spatial organization of a topographic map of sound frequency, called tonotopy (5). Exposure to particular tones (tone-rearing) or language-specific phonemes early in life can shift auditory tuning curves and perception in favor of the experienced acoustic environment at the expense of spectrally neighboring frequencies or speech sound contrasts (6, 7).

Molecular mechanisms underlying critical period plasticity have been most extensively studied for visual acuity (8). In contrast, tonotopic plasticity occurs earlier and for a shorter period of time as compared to the V1 critical period for ocular dominance (9–11). Nevertheless, both critical periods share several features in common. Both auditory and visual cortical plasticity are accompanied by morphological remodeling of dendritic spines (9, 12). Plasticity in A1 emerges earlier than in V1 in close register with accelerated maturation of parvalbumin-positive (PV) cells, shown to be pivotal for critical period onset in V1 (4, 13). Closure of the auditory critical period can be delayed or reopened in adulthood by exposure to continuous broadband noise (0.8 to 30 kHz), which induces several changes in A1 associated with a more plastic state similar to that found in dark-reared V1 (14, 15). Specifically, extended A1 plasticity is associated with decreased PV and BDNF expression, as well as fewer $GABA_A$ α1 and β2/3 subunits (16, 17).

However, compared to the visual system (15, 18), relatively little is known about transcriptional changes occurring during auditory plasticity. The contributions of cell type-specific transcriptional programs to network-level plasticity are poorly understood in A1. For example, it remains unknown to what extent perineuronal nets (PNNs) enwrapping mature PV cells or myelin signaling contribute to the closure of tonotopic plasticity as they do for ocular dominance (19, 20). With the advancement of single-cell RNA sequencing techniques, studies of cortical plasticity are further primed to uncover genetic programs with previously unexplored depth across entire circuits without bias to

Significance

Early life acoustic experience shapes the organization and function of the primary auditory cortex (A1), but molecular mechanisms underlying these critical periods for auditory plasticity are poorly understood. In this study, we use single-nucleus transcriptomics to characterize the multicellular gene expression program in developing A1 and its regulation by tone exposure. We then functionally validated candidate plasticity triggers and brakes to reveal that strengthening of inhibition initiates tonotopic plasticity, while the downstream maturation of myelin-related signaling is associated with critical period closure. These results both confirm conserved mechanisms and identify targets for the regulation of cortical plasticity.

Author contributions: B.T.K., E.E.D., M.E.G., and T.K.H. designed research; B.T.K., T.R.B., E.E.D., and E.J.Z. performed research; B.T.K., T.R.B., E.E.D., and E.J.Z. analyzed data; and B.T.K., E.E.D., M.E.G., and T.K.H. wrote the paper.

Reviewers: D.F.C., Queen Mary University of London; and É.d.V.-S., McGill University.

The authors declare no competing interest.

Data deposition: All sequencing data are available in the Gene Expression Omnibus (GEO) (accession no. GSE140883).

[1]B.T.K., T.R.B., and E.E.D. contributed equally to this work.

[2]Present address: Department of Biomedicine, Basel University, 4056 Basel, Switzerland.

[3]To whom correspondence may be addressed. Email: michael_greenberg@hms.harvard.edu or hensch@mcb.harvard.edu.

This article contains supporting information online at https://www.pnas.org/lookup/suppl/doi:10.1073/pnas.1920433117/-/DCSupplemental.

First published May 13, 2020.

cell type (21, 22). Therefore, we utilized single-nucleus RNA-sequencing (snRNA-seq) in A1 across developmental time points spanning the tonotopic critical period in mice (postnatal days P10, P15, and P20) (9) with normal or altered acoustic experience in order to build a model for gene network changes based on single-cell transcriptomics (23).

Results

Application of snRNA-Seq to the Developing Mouse Auditory Cortex. We performed snRNA-seq to generate a multicellular map of gene expression in A1 at P10, P15, and P20 (Fig. 1*A*). A1 tissue was freshly dissected and flash-frozen, bilateral hemispheres were combined, and nuclei were isolated (Fig. 1*B* and *Materials and Methods*) and then captured, and their mRNA was barcoded using the inDrops platform (21). After initial quality filtering (>500 genes detected per nucleus), the dataset of developmental samples contained 31,293 nuclei, detecting on average 1,913 transcripts (unique molecular identifiers [UMIs]) and 1,244 genes per nucleus (see *SI Appendix*, Fig. S1, for quality control metrics).

Unsupervised clustering analysis identified 29 clusters with distinct transcriptional profiles (22). We used canonical marker genes to classify nuclei into eight main cell types: excitatory neurons (*Slc17a7*+), inhibitory neurons (*Gad1*+), oligodendrocytes (*Olig1*+), astrocytes (*Aqp4*+), endothelial cells (*Cldn5*+), and microglia (*Cx3cr1*+) (Fig. 1*C*). We performed differential gene expression analysis within cell types to explore developmental patterns of transcription across the tonotopic critical period. Genes with a false discovery rate (FDR) <5% were considered statistically significant. In total, we identified hundreds of genes that were dynamically regulated across the auditory tonotopic critical period in all major cortical cell types (Fig. 1*D*). We used gene ontology analysis to broadly classify functional modules of genes that are significantly regulated across this developmental window (Fig. 1*E*). In excitatory neurons, we found that genes associated with vocal learning were enriched for dynamic gene expression across the tonotopic critical period, while genes associated with dendritic transport and GABAergic synaptic transmission were enriched for dynamic gene expression in inhibitory neurons across the same time frame.

To uncover molecular diversity within major cell types, we performed a subclustering analysis, whereby cells classified within one of the main cell types were subjected to principal component analysis to delineate cellular subpopulations. Developmental stage strongly influenced clustering, as excitatory neurons at P10 (precritical period) clustered distinctly from excitatory neurons at P15 and P20 (postcritical period) (*SI Appendix*, Fig. S1*D*). We also found distinct cortical layer-specific clusters, including those belonging to cortical layer V (*Bcl6* and *Kcnn2*+) and layer VI (*Foxp2* and *Ctgf*+) (*SI Appendix*, Fig. S1*E*). We detected a small excitatory neuron cluster that was selectively positive for *Synpr* and *Nr4a2*—genes known to mark the claustrum (*SI Appendix*, Fig. S1*F*) (24). Strikingly, we found that there was a marked increase in immediate early genes, including *c-fos* and *nr4a1*, in the P15/P20 clusters compared to P10 (Fig. 1*F*). This suggests that sensory exposure between P10 and P15/P20 may drive activity-dependent gene expression in the auditory cortex.

Similarly, analysis of interneurons across the P10 to P20 time course revealed clustering predominantly by developmental stage (*SI Appendix*, Fig. S2*A*). Distinct cell populations corresponding to interneuron subtypes were identified, including *Sst*+, *Pvalb*+, *Vip*+, and *Npy*+ cells. We identified a small population of interneurons expressing the serotonin receptor gene *Htr3a*. Our recent work suggests that 5-HT3AR+ interneurons in cortical layer 1 mediate descending thalamocortical disinhibition and that silencing of these interneurons impairs tonotopic plasticity (25). Differential expression analysis between inhibitory cell clusters identified genes enriched within specific interneuron subsets. For example, the neuropeptide gene *Crh* (corticotropin releasing hormone), shown to regulate activity-dependent network plasticity via the integration of new neurons, was expressed predominantly in *Vip*+ interneurons (26).

We performed gene expression analysis within interneurons across early auditory development and found that expression of *Parvalbumin* (*Pvalb*) in interneurons dramatically increased from P10 to P20 (Fig. 1*G*). The maturation of PV-positive, fast-spiking interneurons tightly controls the initiation and termination of critical periods in V1 (27–32). Additionally, we found that genes encoding the Kv3 family of potassium channels that mediate delayed-rectifier currents subserving the high spike rate of fast-spiking interneurons (*Kcnc1* and *Kcnc2*) increased over the same developmental window (*SI Appendix*, Fig. S2*B*) (33–38). The mature $GABA_A$ receptor α1 subunit essential for critical period plasticity in V1 was increased in A1 interneurons from P10 to P15/20 (27). This subunit is enriched at reciprocal, PV–PV, short-range synapses (39). The rise in α1 was matched by a decrease in α5 and α3, a previously characterized developmental subunit switch (39–41). These changes in $GABA_A$ receptor expression mirror those observed in V1 across the critical period for ocular dominance plasticity (42).

Mapping Cell Type-Specific Transcriptional Responses to Tone Rearing. Distorted sensory experience during critical periods has long-lasting effects on circuit development. Repeated tone exposure from P12 to P15 has previously been shown to shift the tonotopic organization of A1 (9, 10) and in other comparable windows across mammals (6). Thus, we sought to identify the transcriptional patterns that underlie this map plasticity by performing snRNA-seq (as above) in A1 of mice that were tone-reared from P12 to P15 and harvested on postnatal days 15 and 20. The dataset for analysis of tone-rearing (including normally reared P15 and P20 samples) included 22,870 nuclei with 1,978 UMIs and 1,391 genes on average per nucleus. Unsupervised clustering analysis identified 19 clusters, representing all major cell types (Fig. 2*A*). We identified hundreds of genes with altered expression (FDR < 5%) in the tone-reared condition in major cell types (Fig. 2*B*). Within each, we found examples of enriched ontologies for genes with expected cell type-specific functions (Fig. 2*C*).

In contrast to the normal developmental trajectory, tone-reared animals displayed altered gene expression patterns in interneurons. For example, *Kcnc1* ($K_v3.1$) exhibited an increase in expression specifically in interneurons immediately following tone-rearing (*SI Appendix*, Fig. S2*B*). $K_v3.1$ is a voltage-gated potassium channel subunit that is responsible for high-frequency action potentials and has been previously shown to be responsive to auditory experience in the brainstem (43). Activity-dependent changes in potassium channel proteins likely contribute to plasticity in the setting of changes in the acoustic environment, such as tone-rearing. In addition to *Kcnc1*, we found that *Nrgn* (neurogranin) and *Calm1* (calmodulin 1) expression increased significantly in tone-reared interneurons (*SI Appendix*, Fig. S2*B*). In neurons, neurogranin is localized to dendritic spines, where it associates with calmodulin (44). Neurogranin overexpression is associated with increased plasticity and long-term potentiation (45). Together, these expression changes in interneurons suggest that tone-rearing drives activity patterns that delay or distort the maturational trajectory of inhibition within A1.

To understand the relationship of GABA signaling to critical period closure, we examined the expression of brake-like factors following altered acoustic experience. We found that the expression of myelin-associated genes (e.g., *Mbp*) was significantly and specifically decreased in tone-reared A1 oligodendrocytes at P15 (Fig. 2*D*). Some genes encoding PNN core proteins (*Bcan* in inhibitory cells) and proteases (*Mme* in inhibitory cells) reversed

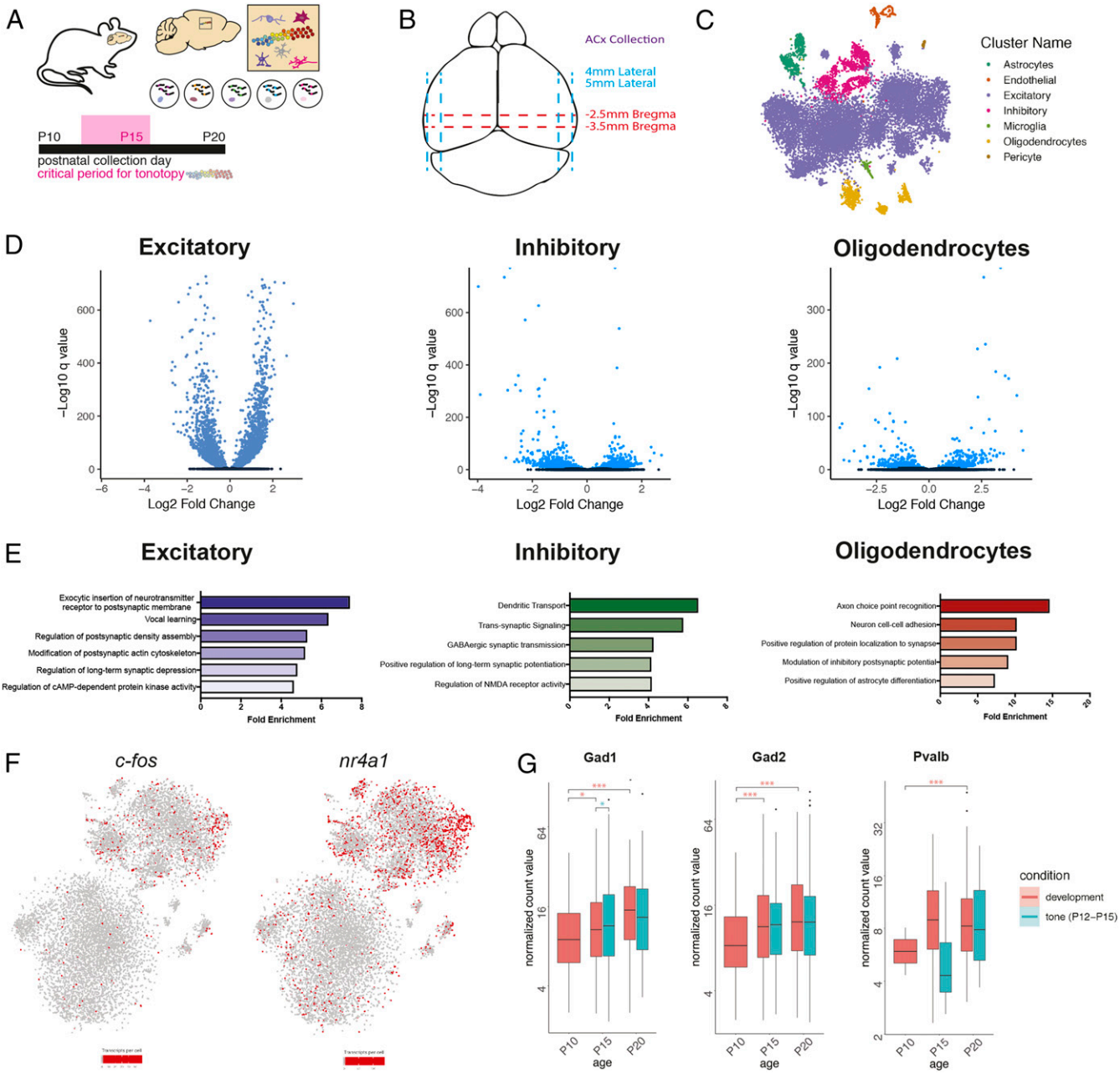

Fig. 1. Single nucleus sequencing of A1 across the tonotopic critical period. (*A*) Schematic of experimental design and time points for tissue collection. (*B*) Diagram of dissection approach used for auditory cortex tissue collection. (*C*) t-SNE plot of cells collected at P10, P15, and P20 under normally reared condition. Colors indicate different cell types. (*D*) Volcano plots depicting differentially expressed genes between P10 and P20 under normally reared conditions in excitatory neurons, inhibitory neurons, and oligodendrocytes. Blue indicates statistically significant genes (FDR < 5%). (*E*) Gene ontology (GO) categories enriched in cell type-specific differentially expressed genes across A1 development. (*F*) t-SNE plots depicting c-fos and nr4a1 expression in P10, P15, and P20 normally reared cells. There is an enrichment of c-fos and nr4a1 positive cells at P20. (*G*) Box plots of the trajectory of average gene expression for *Gad1*, *Gad2*, and *Pvalb* in inhibitory cells from P10 to P20 under conditions of normal development and tone rearing from P12 to P15. Box ranges represent the 25th and 75th percentiles, while the box whiskers indicate the 95% confidence interval. Mean normalized gene expression is indicated. Pairwise gene expression change significance is indicated by asterisks (*FDR < 0.05, ***FDR < 0.001).

their expression pattern in tone-reared animals (Fig. 2*E*). Abundant gene expression changes exhibited by oligodendrocytes suggest they could be key mediators of transiently enhanced map plasticity and delayed critical period closure (19, 20).

One strength of single-nuclear sequencing is the ability to gain novel insight into nonneuronal populations that may have been previously underappreciated. This is particularly important given the growing recognition of the role of nonneuronal cells in circuit development, synapse refinement, and plasticity. However, the role of astrocytes and microglia in the regulation of A1 critical period remains unexplored. In V1, dark-rearing impairs the maturation of astrocytes (46), and the microglial P2Y12 purinergic receptor is required for ocular dominance plasticity (47). Here we found that glia exhibited a distinct transcriptional response to tone-rearing during the tonotopic critical period. Compared to controls, astrocytes from tone-reared animals demonstrated significantly higher expression of immediate-early genes, including *Fos*, *Junb*, and *Nr4a1*, as well as up-regulation of the

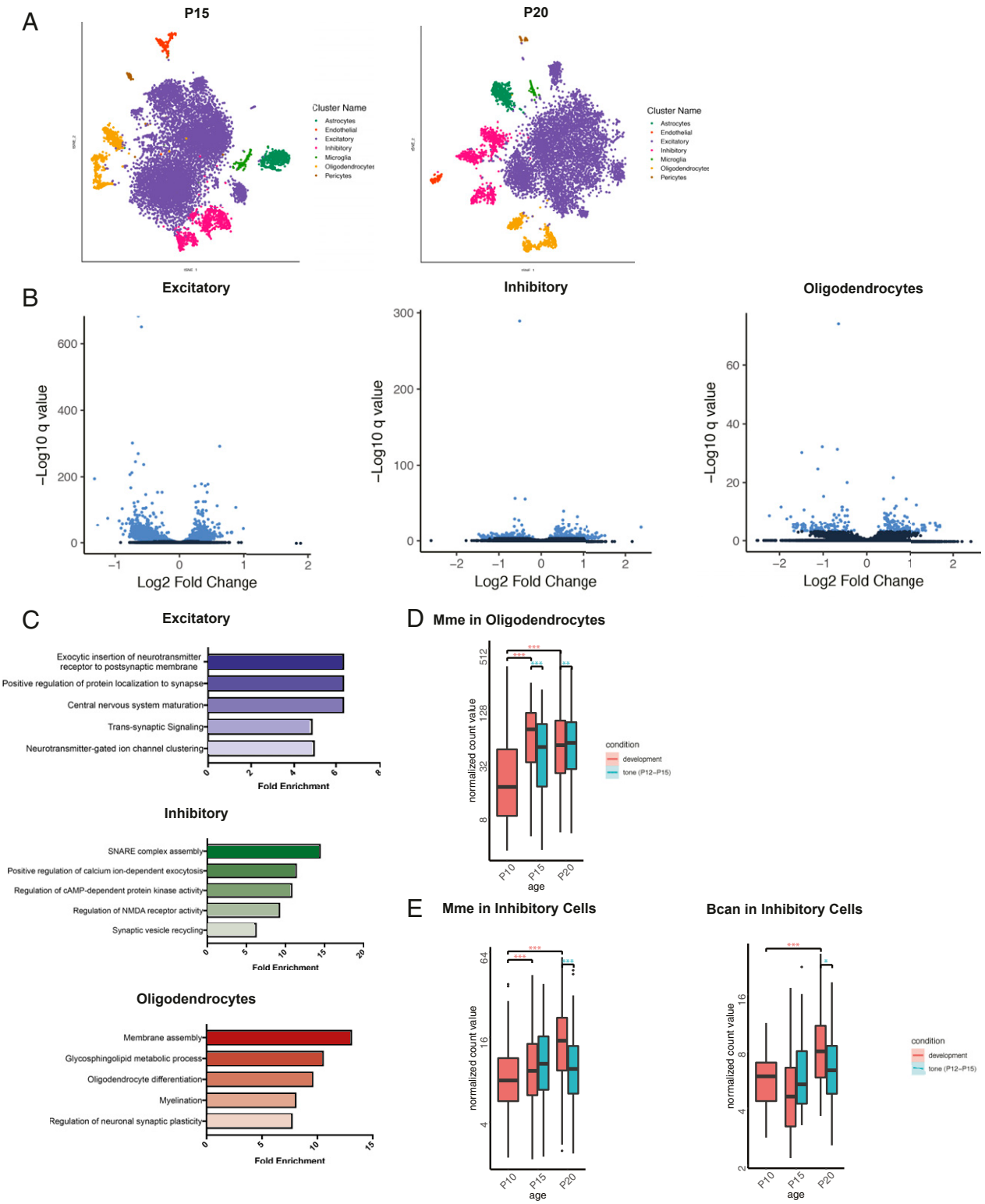

Fig. 2. Cell type-specific effects of tone rearing during the tonotopic critical period. (*A*) t-SNE plots of cells from normally reared and tone reared mice at P15 and P20. (*B*) Volcano plots depicting differentially expressed genes normally reared and tone reared conditions at P15 in excitatory neurons, inhibitory neurons, and oligodendrocytes. Blue indicates statistically significant genes (FDR < 5%). (*C*) Gene ontology (GO) categories enriched in cell type-specific differentially expressed genes at P15 between normally reared and tone reared conditions. (*D*) Boxplot of the trajectory of average gene expression for Mbp from P10 to P20 under conditions of normal development and tone rearing from P12 to P15. Box ranges represent the 25th and 75th percentiles, while the box whiskers indicate the 95% confidence interval. Mean normalized gene expression is indicated. Pairwise gene expression change significance is indicated by asterisks (**FDR < 0.01, ***FDR < 0.001). (*E*) Boxplot of the trajectory of average gene expression for Mme and Bcan from P10 to P20 under conditions of normal development and tone rearing from P12 to P15. Box ranges represent the 25th and 75th percentiles, while the box whiskers indicate the 95% confidence interval. Mean normalized gene expression is indicated. Pairwise gene expression change significance is indicated by asterisks (*FDR < 0.05, ***FDR < 0.001).

Notch1 target *Hes5*. Notch signaling is thought to be important for neural activity-driven astrocyte maturation and morphological response to stimuli (48, 49).

The excitatory amino acid transporter *Slc1a3*, as well as the *Kcnn2* small conductance calcium-activated channel, were both down-regulated in tone-reared astrocytes, perhaps as a result of an activity-dependent compensatory mechanism. Analysis of gene expression in microglia was limited by small cell numbers, but those from tone-reared mice demonstrated a nearly fourfold reduction in complement gene *C1qb* and Fc-receptor–like molecule *Fcrls*, both of which are typically down-regulated upon microglial activation (50, 51). Additional studies are needed to define the functional significance of specific glial populations to auditory development and plasticity.

Functional Implications of Inhibitory Maturation. Extensive work in V1 has shown the functional maturation of GABAergic innervation is an important driver of critical period progression (52). In the absence of GAD65, a key GABA biosynthetic enzyme, a permanent precritical period state persists in V1 (53). Plasticity can be rescued by administration of Diazepam, a benzodiazepine agonist which enhances particular $GABA_A$ receptor currents such that residual GABA levels in the absence of GAD65 drive sufficient inhibitory transmission. For example, while GAD65 knockout mice do not exhibit a shift in ocular dominance following brief monocular deprivation, these mice can exhibit plasticity at any age when treated with Diazepam (54).

Our data showed that expression of *Gad1* and *Gad2*, encoding the two GABA synthetic enzymes GAD67 and GAD65, respectively, increased over development in A1 interneurons (Fig. 1*G*). One further theme that emerged from our A1 snRNA-seq data was the dynamic nature of inhibitory receptors across the tonotopic critical period. This suggests that the maturation of inhibitory tone may also be important for critical period timing in the developing auditory cortex. We, therefore, examined how broad manipulation of inhibitory transmission might affect A1 topography and plasticity using voltage-sensitive dye imaging (9).

Functional thalamocortical connectivity can be measured in an acute slice preparation, where focal stimulation to single sites in auditory thalamus (ventral medial geniculate body [MGBv]) elicits topographic responses in A1 (Fig. 3*A*). Our previous work revealed that prior to the critical period at P10, focal electrical stimulation of medial MGBv sites (which receive high auditory frequency input in vivo) is more effective at driving A1 responses than lateral, low-auditory frequency sites (9). This bias is gradually lost over critical period development, with stimulation at all sites in MGBv eliciting similar maximal responses at topographic locations across A1. In GAD65 knockout animals, this maturation failed to occur, and rostral sites continued to show greater activation beyond the normal developmental window (Fig. 3*B*). Furthermore, in wild-type (WT) mice over early development, stimulation to single sites in MGBv typically yielded progressively shorter latency responses, translocating from layer VI to layer IV (Fig. 3 *C* and *D*). In GAD65 knockout mice, the site of shortest latency remained in deeper layer VI despite an overall shortening of response latencies comparable to WT animals (Fig. 3*D*).

To test whether GAD65 is essential for the onset of the tonotopic critical period, knockout mice were reared under repeated 7-kHz tones between P12 and P15, which typically yields a shift in the tonotopic map and thalamocortical functional connectivity in control mice (Fig. 4 *A* and *B*) (9). The relationship between the stimulus site in MGBv and the site of maximal response in A1 is defined as the topographic slope and is equal to 1 in control animals but drops in animals tone-reared during the critical period (Fig. 4 *B* and *C*) (9). Mice lacking GAD65 failed to shift their topographic functional connectivity (Fig. 4 *B* and *C*) unless pretreated with Diazepam (Fig. 4*D*), consistent with the hypothesis that their critical period onset is delayed (Fig. 3*D*). Tone exposure during a more extended time frame—from P8 to P20—also did not alter the tonotopic map in GAD65 null mice (Fig. 4*C*). In WT animals, administration of Diazepam given prior to the natural critical period was also effective at driving plasticity (Fig. 4*E*), shifting plasticity earlier and preventing it during the expected window (Fig. 4*F*). These results collectively demonstrate that the development of inhibitory tone is necessary for the onset of critical period plasticity in A1, as it is in V1.

Molecular Brakes on Auditory Plasticity. In order to solidify changes made to sensory maps during the critical period, molecular brakes turn on to actively close the window and prevent further circuit refinements (55). Brakes are endogenous factors that halt or restrict plasticity, such as the maturation of the extracellular matrix as a structural barrier to circuit rewiring. We found that the expression of PNN-related genes, including proteoglycans and proteases, were dynamically regulated across A1 development and in response to tone exposure (Fig. 2*E*). Notably, chondroitin sulfate proteoglycans (CSPGs) tightly enwrap PV basket cells in the form of PNNs (19, 56). PNN intensity, as revealed by *Wisteria Floribunda Agglutinin* (WFA) labeling, increased in A1 from P10 to P20 (Fig. 5 *A* and *D*, *Left*).

Another example of a molecular brake is the increased myelination of axons in cortex, which limits axon regrowth potential and synaptic plasticity (57). Myelin-related gene expression and intracortical myelin basic protein (MBP) staining in WT mice increased dramatically across this 10-d window (Fig. 5 *A* and *C*, *Left*). The GAD65 knockout animals displayed lower gray matter staining intensity for both WFA and myelin (Fig. 5 *C* and *D*, *Right*), consistent with the shortest latency thalamocortical responses remaining in layer VI (Fig. 3*D*). Diazepam treatment, which enabled normal tonotopic plasticity (Fig. 4*F*), did not fully rescue PNN intensity by P20 (Fig. 5*D*) but returned myelin signals to WT levels (Fig. 5*C*). Thus, myelination may serve as an earlier signal for map consolidation.

Much of the myelin-related brakes on plasticity have been attributed to signaling through the Nogo receptor, NgR (58). The neurite outgrowth inhibitor Nogo-A (Rtn4), which signals through NgR, was up-regulated by oligodendrocytes at P20 (*SI Appendix*, Fig. S2*C*) but down-regulated in *Tubb3*+ neurons (59) after the critical period, which was prevented by tone-rearing (Fig. 5 *E* and *F*). This suggests a dynamic interplay between neuronal and glial populations to regulate both the level and timing of plasticity within cortical circuits.

Conveniently, the NgR is a key mediator of the downstream response to several brake-like factors, including CSPGs, myelin factors, and Nogo-A (Fig. 5*G*) (60). We thus examined whether the degree or timing of map plasticity in A1 might be altered by loss of this receptor. We found that NgR knockout animals were plastic during both the normal critical period and beyond (Fig. 5*H*). Thus, myelin/CSPG-mediated signaling via the NgR is necessary to restrict plasticity at the end of the tonotopic critical period in A1. A permissive environment for structural changes in the absence of NgR would allow a prolonged window for anatomical consolidation of functional refinements.

Discussion

Early postnatal acoustic experience shapes the structural and functional organization of the auditory system (7). Neural activity during narrowly defined critical periods drives frequency selectivity and tonotopic organization. Our study sought to characterize the cell type-specific transcriptional underpinnings of this carefully orchestrated multicellular collaboration. We observed gene expression changes in all major cell types across early A1 development, during which these sensory-driven circuit refinements occur. In addition to the vast transcriptomic resource created in this study, we also extend findings from the

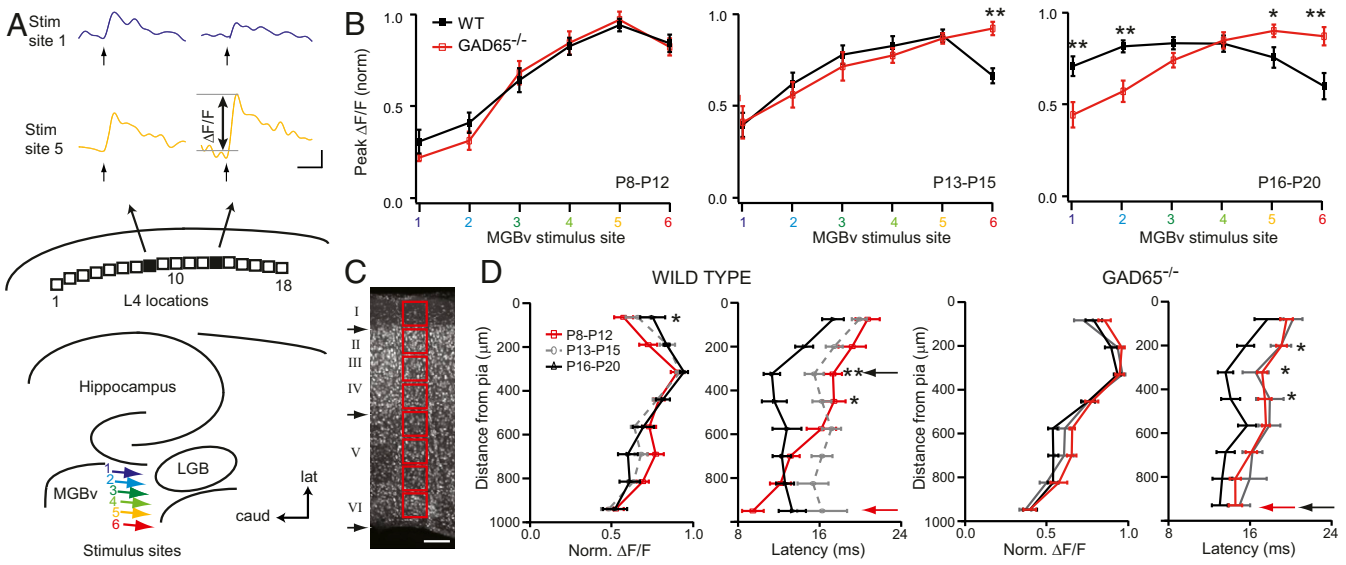

Fig. 3. Delayed thalamocortical maturation in GAD65-deficient mice. (*A*) Schematic of the six MGBv stimulus sites (colored arrows) and 18 L4 locations analyzed. Sample voltage-sensitive dye imaging (VSDI) traces of maximum change in fluorescence (ΔF/F) at two different L4 locations (locations 8 and 13) as a function of time following a single, 1-ms stimulus pulse to MGBv site 1 (blue) or 5 (yellow) in a P12 WT mouse. LGB, lateral geniculate body. (Scale bars, 100 ms and 0.1% ΔF/F.) (*B*) Normalized peak ΔF/F as a function of stimulus site for WT (black) and *GAD65*$^{-/-}$ (red), respectively, for three age groups (P8 to P12, $n = 13, 7$; P13 to P15, $n = 16, 9$; and P16 to P20, $n = 16, 13$). (*C*) Nissl stain of a P20 thalamocortical slice for columnar analysis (red square). Black arrows denote approximate borders between layers LI/II, LIV/V, and LVI/white matter. Normalized ΔF/F with distance from pia for WT and GAD65$^{-/-}$ mice at three age groups (red, P8 to P12, $n = 13, 8$; gray, P13 to P15, $n = 15, 9$; and black, P16 to P20, $n = 11, 13$). (Scale bar, 125 μm.) (*D*) Normalized ΔF/F with latency from pia for the same groups. Red and black arrows denote location of shortest latency in P8 to P12 and P16 to P20 mice, respectively. Note the shift of shortest latency from LVI to LIV in WT mice is not seen in GAD65$^{-/-}$ mice across this age range. $*P < 0.05$; $**P < 0.01$, two-way ANOVA with post hoc Bonferroni correction; mean ± SEM.

visual system to the auditory cortex. Specifically, we demonstrate that GAD65, a key synthetic enzyme for GABA, and the Nogo receptor, a mediator of myelin/CSPG signaling, are both necessary for proper critical period onset and offset, respectively (20, 53). These results underscore conserved mechanisms for the regulation of cortical plasticity.

Our study further reveals an activity-dependent mobilization of molecular machinery enabling plasticity. Thus, tone-rearing

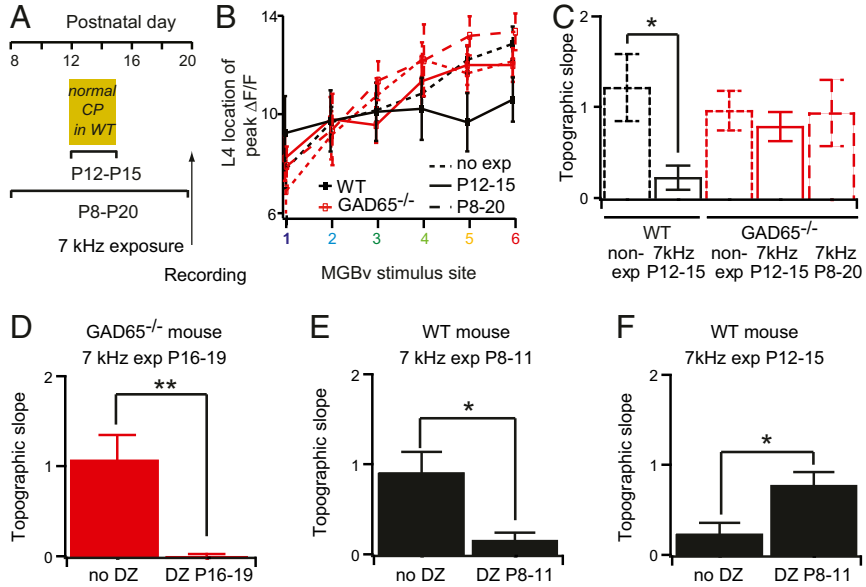

Fig. 4. Critical period onset reflects excitatory–inhibitory balance in A1. (*A*) Schedule for tone exposure window and recording (arrows). (*B*) Location of L4 peak ΔF/F in response to different MGBv stimulus sites for mice nonexposed ($n = 9$ for WT, 12 for *GAD65*$^{-/-}$) or exposed to 7 kHz between P12 and P15 ($n = 8$ for WT, 12 for *GAD65*$^{-/-}$) or P8 and P20 ($n = 6$ for *GAD65*$^{-/-}$). (*C*) Corresponding topographic slopes (slopes of the curves in *C*). (*D–F*) Topographic slopes for (*D*) *GAD65*$^{-/-}$ mice exposed to 7 kHz between P16 and P19 with (DZ P16 to 19, $n = 8$) or without (no DZ, $n = 9$) DZ injection between P16 and P19, (*E*) WT mice exposed to 7 kHz between P8 and P11 with (DZ P8 and P11, $n = 8$) or without (no DZ, $n = 8$) DZ injection between P8 and P11, and (*F*) WT mice exposed to 7 kHz between P12 and P15 with (DZ P8 and P11, $n = 8$) or without (no DZ, $n = 9$) DZ injection between P8 and P11. $*P < 0.05$; $**P < 0.01$; *t* test; mean ± SEM.

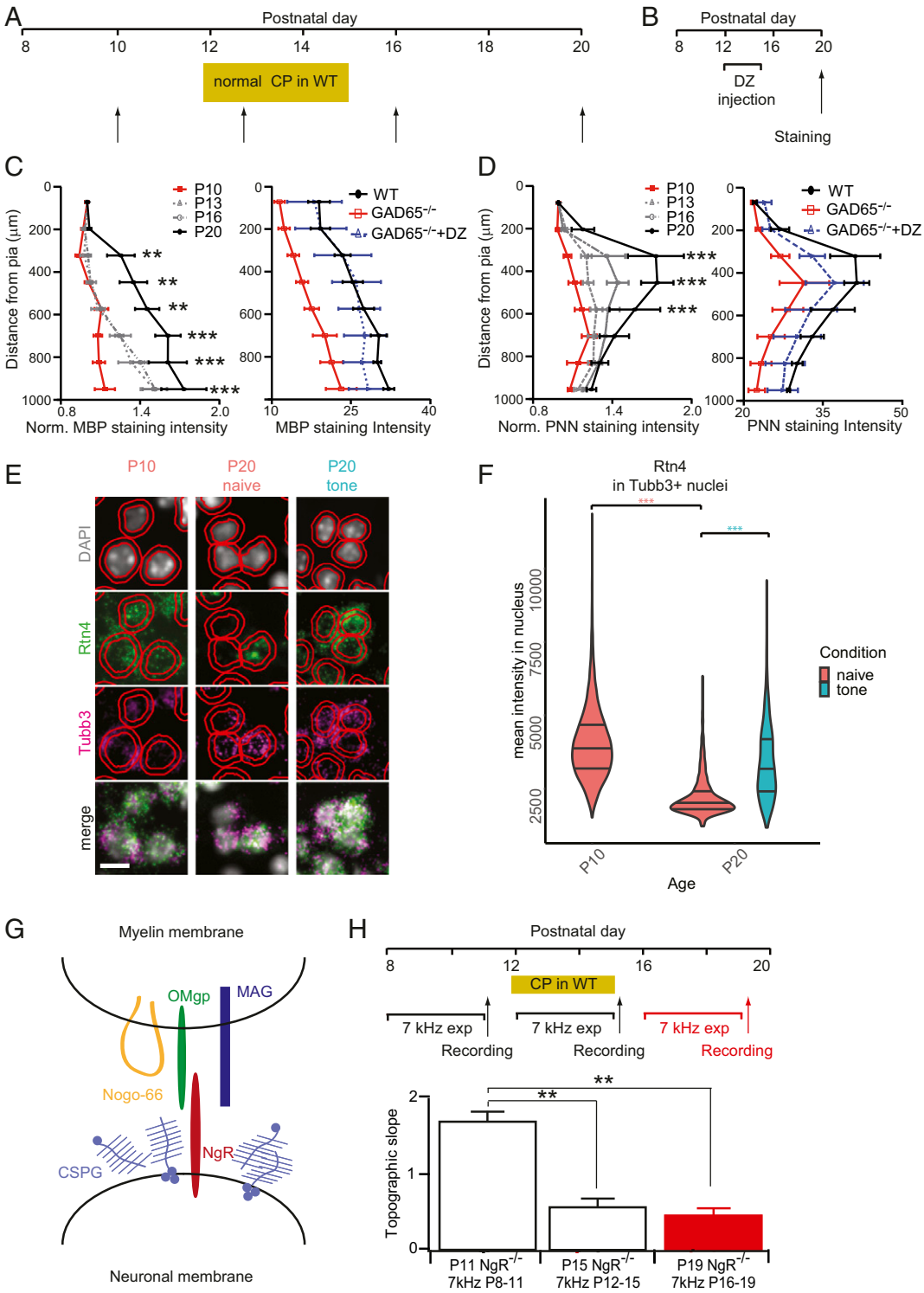

Fig. 5. Critical period closure in A1 signaled by myelin/PNN formation and NgR. (*A*) Schedule for staining (arrows) with reference to typical A1 critical period in WT mice. (*B*) Schedule for staining (arrows) with reference to Diazepam or vehicle treatment in *GAD65*$^{-/-}$ mice. (*C* and *D*) (*Left*) Quantification of relative MBP (*C*) and WFA (*D*) staining intensity in P10 ($n = 5, 4$), P13 ($n = 5, 4$), P16 ($n = 4, 4$), and P20 ($n = 4, 4$) WT mice. $^{**}P < 0.01$ $^{***}P < 0.001$, two-way ANOVA with post hoc Bonferroni correction; mean ± SEM. (*Right*) Quantification of MBP (*C*) and PNN (*D*) staining in P20 WT nonexposed (black, $n = 4, 4$), *GAD65*$^{-/-}$ (red, $n = 5, 3$) and *GAD65*$^{-/-}$ injected with DZ between P12-P15 (blue dashed, $n = 5, 4$). $^{*}P < 0.05$; $^{**}P < 0.01$, two-way ANOVA with post hoc Bonferroni correction; mean ± SEM. (*E*) Fluorescent in situ hybridization (FISH) in A1 labeling cellular nuclei (*DAPI*), Nogo-A (*Rtn4*), neuronal marker (*Tubb3*), and their merged images across ages and tone-rearing. Representative images are from Layer V/VI. Red outlines are QuPath (67) segmented nuclei and an expanded estimated cell border. (Scale bar, 10 μm.) (*F*) Quantification of mean FISH signal intensity in Tubb3+ nuclei (*Materials and Methods*) at P10, P20, and P20 after tone-rearing during the critical period (P12 to P15). Quantification was averaged across all layers. $^{***}P < 0.001$, Kruskal–Wallis rank sum test with post hoc Dunn test; horizontal lines in violin plot indicate quantiles 0.25, 0.50, and 0.75. (*G*) Schematic of putative NgR ligands in myelin membrane (Nogo-66, OMgp, and MAG) and the extracellular matrix (CSPG). (*H*) Schedule for sound exposure and VSDI recordings (arrows). Topographic slopes for *NgR*$^{-/-}$ mice exposed to 7 kHz between P8 and P11 (P11, white, $n = 5$), between P12 and P15 (P15, white, $n = 8$) or between P16 and P19 (P19, red, $n = 4$). $^{**}P < 0.01$, *t* test; mean ± SEM.

per se altered normal developmental trajectories of both GABAergic circuits and structural barriers to plasticity such as myelination and PNNs. The idea that abnormal acoustic experience during the critical period alters maturation trajectories has been suggested by other studies. For example, $GABA_B$-mediated inhibitory long-term depression (iLTD) is triggered by prepost pairing of action potentials at PV-to-principal cell synapses during the A1 critical period, which is thought to underlie a disinhibitory mechanism permissive for plasticity (61). This iLTD switches to potentiation (iLTP) as development proceeds.

After tone-rearing, the number of cells responsive to the rearing frequency increases in a topographic zone of A1, and they exhibit a premature switch to iLTP (61). Instead, our data from A1 biopsies show that the gene encoding $GABA_B$ subunit 2 normally decreases over early development but increases in tone-reared animals, which should mediate continued iLTD. One possibility is that tone-rearing drives both iLTP and iLTD in a topographic manner to mediate map expansion to the rearing frequency and compensatory retraction in others. In addition, presynaptic $GABA_B$ receptors have been shown to regulate the experience-dependent switch from depression to facilitation in inhibitory plasticity (62).

The auditory system is a tractable model of experience-dependent plasticity due, in part, to its topographic organization. The use of snRNA-seq allows for the dissection of layer-specific excitatory cell types and classes of inhibitory neurons, as well as nonneuronal cells. However, this approach homogenizes the tonotopic organization of cells in A1. It is not clear whether distortion of inhibitory maturation or molecular brake onset occurs within the tone-responsive areas of cortex in response to overstimulation or if the neighboring part of the tonotopic map is silenced in a competitive manner. Future studies could use multiplexed fluorescence in situ hybridization to visualize spatially restricted cell type-specific transcriptional changes to address these questions.

Our data represent a significant advance over existing resources as this study profiles transcription with cell type specificity across time and with critical period perturbation. However, the use of snRNA-seq also has several limitations. First, this approach has low capture efficiency, such that a small proportion of a cell's total transcriptome is represented in the final sequenced library. This challenge makes it difficult to distinguish between biologic variability and technical noise for low-abundance transcripts, such as the nicotinic acetylcholine brake Lynx1 (25).

The low amount of input material also leads to high levels of technical noise, again making it difficult to observe biologic variation. Owing to low capture efficiency and stochastic gene expression, gene dropout (where gene expression is zero in a given cell) is quite common, leading to zero-inflated expression data. Other potential sources of bias include the tissue dissociation method, as enzymatic treatments may affect cell viability, as well as the low number of animals from which nuclei were collected. The relative merits of single-cell sequencing, as opposed to bulk RNA sequencing, depend on many factors, including the specific scientific question, cell type abundance, and gene-of-interest expression level.

Despite these limitations, snRNA-seq is an important discovery tool with which to obtain previously impossible degrees of cellular resolution. For example, we found that *Nrgn* is upregulated in tone-reared interneurons (*SI Appendix*, Fig. S2*B*), while this gene is restricted to principal cells in the mature cortex across species (63). There is precedent that *Nrgn* can be transiently expressed in GABAergic interneurons in a developmentally restricted fashion (64) and in subsets of GABAergic neurons in other contexts (65). Similarly, $K_v3.1$ may be transiently expressed in oligodendrocyte precursor cells at even earlier ages (66). This highlights the importance of unbiased examination of longitudinal trajectories of dynamic gene expression across cell types. Overall, our results are consistent with a pivotal role for PV+ circuits in regulating critical period profiles across brain regions (32). The transcriptomic data obtained in the present study provide insights into critical period regulation and a resource for future investigation into cell type-specific regulatory mechanisms in auditory cortex development.

Materials and Methods

All experiments using animals were performed according to protocols approved by the Harvard University Institutional Animal Care and Use Committee. Tone rearing was performed between postnatal days 12 to 15, and litters were moved back to standard housing on postnatal day 16. The auditory cortex was dissected and flash frozen; a nuclear suspension was subsequently prepared using gradient centrifugation. Single nuclei were captured, barcoded, and sequenced according to the inDrops technique as previously described (21). All sequencing data are available in the Gene Expression Omnibus (GSE140883). Voltage-sensitive dye imaging of C57BL/6J, $GAD65^{-/-}$, or $NgR^{-/-}$ mice was performed on acutely prepared auditory thalamocortical slices, as described previously (5, 9). Additional details are contained in *SI Appendix, Extended Experimental Procedures*.

ACKNOWLEDGMENTS. We thank members of the M.E.G. and T.K.H. laboratories for discussions and critical reading of the manuscript. We thank Mari Nakamura, MSc, for expert mouse colony maintenance and Marykate O'Malley, MSc, BSN, RN, for her assistance with figures. We thank the Neurobiology Department and Neurobiology Imaging Facility for consultation and instrument availability supported in part by the Neural Imaging Center as part of an National Institute of Neurological Disorders and Stroke P30 Core Center grant NS072030. We further thank the Single Cell Core at Harvard Medical School, Boston, MA, for performing the single-cell RNA-Seq sample preparation. This work was funded by NIH grant R01 NS028829 to M.E.G., a Pediatric Scientist Development Award and March of Dimes funding to B.T.K., the Harvard Society of Fellows to T.R.B., Thomas T. Hoopes Prize to E.J.Z., and a National Institute of Mental Health Silvio Conte Center (P50MH094271) and World Premier International Research Center for Neurointelligence (Japan Society for the Promotion of Science) grant to T.K.H.

1. T. K. Hensch, Critical period regulation. *Annu. Rev. Neurosci.* **27**, 549–579 (2004).
2. L. C. Katz, C. J. Shatz, Synaptic activity and the construction of cortical circuits. *Science* **274**, 1133–1138 (1996).
3. T. K. Hensch, Critical period mechanisms in developing visual cortex. *Curr. Top. Dev. Biol.* **69**, 215–237 (2005).
4. A. E. Takesian, T. K. Hensch, Balancing plasticity/stability across brain development. *Prog. Brain Res.* **207**, 3–34 (2013).
5. T. A. Hackett, T. R. Barkat, B. M. J. O'Brien, T. K. Hensch, D. B. Polley, Linking topography to tonotopy in the mouse auditory thalamocortical circuit. *J. Neurosci.* **31**, 2983–2995 (2011).
6. C. E. Schreiner, D. B. Polley, Auditory map plasticity: Diversity in causes and consequences. *Curr. Opin. Neurobiol.* **24**, 143–156 (2014).
7. J. F. Werker, T. K. Hensch, Critical periods in speech perception: New directions. *Annu. Rev. Psychol.* **66**, 173–196 (2015).
8. T. K. Hensch, E. M. Quinlan, Critical periods in amblyopia. *Vis. Neurosci.* **35**, E014 (2018).
9. T. R. Barkat, D. B. Polley, T. K. Hensch, A critical period for auditory thalamocortical connectivity. *Nat. Neurosci.* **14**, 1189–1194 (2011).
10. E. de Villers-Sidani, E. F. Chang, S. Bao, M. M. Merzenich, Critical period window for spectral tuning defined in the primary auditory cortex (A1) in the rat. *J. Neurosci.* **27**, 180–189 (2007).
11. H. Morishita, T. K. Hensch, Critical period revisited: Impact on vision. *Curr. Opin. Neurobiol.* **18**, 101–107 (2008).
12. N. Mataga, Y. Mizuguchi, T. K. Hensch, Experience-dependent pruning of dendritic spines in visual cortex by tissue plasminogen activator. *Neuron* **44**, 1031–1041 (2004).
13. J. A. del Río, L. de Lecea, I. Ferrer, E. Soriano, The development of parvalbumin-immunoreactivity in the neocortex of the mouse. *Brain Res. Dev. Brain Res.* **81**, 247–259 (1994).
14. M. Fagiolini, T. Pizzorusso, N. Berardi, L. Domenici, L. Maffei, Functional postnatal development of the rat primary visual cortex and the role of visual experience: Dark rearing and monocular deprivation. *Vision Res.* **34**, 709–720 (1994).
15. D. Tropea *et al.*, Gene expression changes and molecular pathways mediating activity-dependent plasticity in visual cortex. *Nat. Neurosci.* **9**, 660–668 (2006).
16. X. Zhou, R. Panizzutti, E. de Villers-Sidani, C. Madeira, M. M. Merzenich, Natural restoration of critical period plasticity in the juvenile and adult primary auditory cortex. *J. Neurosci.* **31**, 5625–5634 (2011).
17. E. de Villers-Sidani, K. L. Simpson, Y.-F. Lu, R. C. S. Lin, M. M. Merzenich, Manipulating critical period closure across different sectors of the primary auditory cortex. *Nat. Neurosci.* **11**, 957–965 (2008).

18. M. Majdan, C. J. Shatz, Effects of visual experience on activity-dependent gene regulation in cortex. *Nat. Neurosci.* **9**, 650–659 (2006).
19. T. Pizzorusso *et al*., Reactivation of ocular dominance plasticity in the adult visual cortex. *Science* **298**, 1248–1251 (2002).
20. A. W. McGee, Y. Yang, Q. S. Fischer, N. W. Daw, S. M. Strittmatter, Experience-driven plasticity of visual cortex limited by myelin and Nogo receptor. *Science* **309**, 2222–2226 (2005).
21. A. M. Klein *et al*., Droplet barcoding for single-cell transcriptomics applied to embryonic stem cells. *Cell* **161**, 1187–1201 (2015).
22. E. Z. Macosko *et al*., Highly parallel genome-wide expression profiling of individual cells using nanoliter droplets. *Cell* **161**, 1202–1214 (2015).
23. B. Lacar *et al*., Nuclear RNA-seq of single neurons reveals molecular signatures of activation. *Nat. Commun.* **7**, 11022 (2016).
24. D. Binks, C. Watson, L. Puelles, A re-evaluation of the anatomy of the claustrum in rodents and primates—Analyzing the effect of pallial expansion. *Front. Neuroanat.* **13**, 34 (2019).
25. A. E. Takesian, L. J. Bogart, J. W. Lichtman, T. K. Hensch, Inhibitory circuit gating of auditory critical-period plasticity. *Nat. Neurosci.* **21**, 218–227 (2018).
26. I. Garcia *et al*., Local CRH signaling promotes synaptogenesis and circuit integration of adult-born neurons. *Dev. Cell* **30**, 645–659 (2014).
27. M. Fagiolini *et al*., Specific GABAA circuits for visual cortical plasticity. *Science* **303**, 1681–1683 (2004).
28. J. L. Hanover, Z. J. Huang, S. Tonegawa, M. P. Stryker, Brain-derived neurotrophic factor overexpression induces precocious critical period in mouse visual cortex. *J. Neurosci.* **19**, RC40 (1999).
29. Z. J. Huang *et al*., BDNF regulates the maturation of inhibition and the critical period of plasticity in mouse visual cortex. *Cell* **98**, 739–755 (1999).
30. S. J. Kuhlman *et al*., A disinhibitory microcircuit initiates critical-period plasticity in the visual cortex. *Nature* **501**, 543–546 (2013).
31. S. Sugiyama *et al*., Experience-dependent transfer of Otx2 homeoprotein into the visual cortex activates postnatal plasticity. *Cell* **134**, 508–520 (2008).
32. H. H. C. Lee *et al*., Genetic Otx2 mis-localization delays critical period plasticity across brain regions. *Mol. Psychiatry* **22**, 680–688 (2017).
33. G. Baranauskas, T. Tkatch, K. Nagata, J. Z. Yeh, D. J. Surmeier, Kv3.4 subunits enhance the repolarizing efficiency of Kv3.1 channels in fast-spiking neurons. *Nat. Neurosci.* **6**, 258–266 (2003).
34. J. Du, L. Zhang, M. Weiser, B. Rudy, C. J. McBain, Developmental expression and functional characterization of the potassium-channel subunit Kv3.1b in parvalbumin-containing interneurons of the rat hippocampus. *J. Neurosci.* **16**, 506–518 (1996).
35. A. Erisir, D. Lau, B. Rudy, C. S. Leonard, Function of specific K(+) channels in sustained high-frequency firing of fast-spiking neocortical interneurons. *J. Neurophysiol.* **82**, 2476–2489 (1999).
36. C.-C. Lien, P. Jonas, Kv3 potassium conductance is necessary and kinetically optimized for high-frequency action potential generation in hippocampal interneurons. *J. Neurosci.* **23**, 2058–2068 (2003).
37. B. W. Okaty, M. N. Miller, K. Sugino, C. M. Hempel, S. B. Nelson, Transcriptional and electrophysiological maturation of neocortical fast-spiking GABAergic interneurons. *J. Neurosci.* **29**, 7040–7052 (2009).
38. B. Rudy, C. J. McBain, Kv3 channels: Voltage-gated K+ channels designed for high-frequency repetitive firing. *Trends Neurosci.* **24**, 517–526 (2001).
39. M. Strüber, P. Jonas, M. Bartos, Strength and duration of perisomatic GABAergic inhibition depend on distance between synaptically connected cells. *Proc. Natl. Acad. Sci. U.S.A.* **112**, 1220–1225 (2015).
40. D. D. Dunning, C. L. Hoover, I. Soltesz, M. A. Smith, D. K. O'Dowd, GABA(A) receptor-mediated miniature postsynaptic currents and alpha-subunit expression in developing cortical neurons. *J. Neurophysiol.* **82**, 3286–3297 (1999).
41. A. M. Lavoie, J. J. Tingey, N. L. Harrison, D. B. Pritchett, R. E. Twyman, Activation and deactivation rates of recombinant GABA(A) receptor channels are dependent on alpha-subunit isoform. *Biophys. J.* **73**, 2518–2526 (1997).
42. K. Heinen *et al*., GABAA receptor maturation in relation to eye opening in the rat visual cortex. *Neuroscience* **124**, 161–171 (2004).
43. J. G. Strumbos, D. B. Polley, L. K. Kaczmarek, Specific and rapid effects of acoustic stimulation on the tonotopic distribution of Kv3.1b potassium channels in the adult rat. *Neuroscience* **167**, 567–572 (2010).
44. A. Petersen, N. Z. Gerges, Neurogranin regulates CaM dynamics at dendritic spines. *Sci. Rep.* **5**, 11135 (2015).
45. L. Zhong *et al*., Increased prefrontal cortex neurogranin enhances plasticity and extinction learning. *J. Neurosci.* **35**, 7503–7508 (2015).
46. C. M. Müller, Dark-rearing retards the maturation of astrocytes in restricted layers of cat visual cortex. *Glia* **3**, 487–494 (1990).
47. G. O. Sipe *et al*., Microglial P2Y12 is necessary for synaptic plasticity in mouse visual cortex. *Nat. Commun.* **7**, 10905 (2016).
48. E. Acaz-Fonseca, A. Ortiz-Rodriguez, I. Azcoitia, L. M. Garcia-Segura, M.-A. Arevalo, Notch signaling in astrocytes mediates their morphological response to an inflammatory challenge. *Cell Death Discov.* **5**, 85 (2019).
49. P. Hasel *et al*., Neurons and neuronal activity control gene expression in astrocytes to regulate their development and metabolism. *Nat. Commun.* **8**, 15132 (2017).
50. M. L. Bennett *et al*., New tools for studying microglia in the mouse and human CNS. *Proc. Natl. Acad. Sci. U.S.A.* **113**, E1738–E1746 (2016).
51. C. Sousa *et al*., Single-cell transcriptomics reveals distinct inflammation-induced microglia signatures. *EMBO Rep.* **19**, e46171 (2018).
52. T. K. Hensch, Critical period plasticity in local cortical circuits. *Nat. Rev. Neurosci.* **6**, 877–888 (2005).
53. T. K. Hensch *et al*., Local GABA circuit control of experience-dependent plasticity in developing visual cortex. *Science* **282**, 1504–1508 (1998).
54. M. Fagiolini, T. K. Hensch, Inhibitory threshold for critical-period activation in primary visual cortex. *Nature* **404**, 183–186 (2000).
55. D. Bavelier, D. M. Levi, R. W. Li, Y. Dan, T. K. Hensch, Removing brakes on adult brain plasticity: From molecular to behavioral interventions. *J. Neurosci.* **30**, 14964–14971 (2010).
56. W. Härtig *et al*., Cortical neurons immunoreactive for the potassium channel Kv3.1b subunit are predominantly surrounded by perineuronal nets presumed as a buffering system for cations. *Brain Res.* **842**, 15–29 (1999).
57. M. E. Schwab, S. M. Strittmatter, Nogo limits neural plasticity and recovery from injury. *Curr. Opin. Neurobiol.* **27**, 53–60 (2014).
58. V. Pernet, Nogo-A in the visual system development and in ocular diseases. *Biochim. Biophys. Acta Mol. Basis Dis.* **1863**, 1300–1311 (2017).
59. M. K. Lee, J. B. Tuttle, L. I. Rebhun, D. W. Cleveland, A. Frankfurter, The expression and posttranslational modification of a neuron-specific beta-tubulin isotype during chick embryogenesis. *Cell Motil. Cytoskeleton* **17**, 118–132 (1990).
60. T. L. Dickendesher *et al*., NgR1 and NgR3 are receptors for chondroitin sulfate proteoglycans. *Nat. Neurosci.* **15**, 703–712 (2012).
61. E. D. Vickers *et al*., Parvalbumin-interneuron output synapses show spike-timing-dependent plasticity that contributes to auditory map remodeling. *Neuron* **99**, 720–735.e6 (2018).
62. A. E. Takesian, V. C. Kotak, D. H. Sanes, Presynaptic GABA(B) receptors regulate experience-dependent development of inhibitory short-term plasticity. *J. Neurosci.* **30**, 2716–2727 (2010).
63. I. Singec, R. Knoth, M. Ditter, B. Volk, M. Frotscher, Neurogranin is expressed by principal cells but not interneurons in the rodent and monkey neocortex and hippocampus. *J. Comp. Neurol.* **479**, 30–42 (2004).
64. S. Gribaudo *et al*., Transitory and activity-dependent expression of neurogranin in olfactory bulb tufted cells during mouse postnatal development. *J. Comp. Neurol.* **520**, 3055–3069 (2012).
65. M. Simat, F. Parpan, J.-M. Fritschy, Heterogeneity of glycinergic and gabaergic interneurons in the granule cell layer of mouse cerebellum. *J. Comp. Neurol.* **500**, 71–83 (2007).
66. S. Tiwari-Woodruff *et al*., K+ channel KV3.1 associates with OSP/claudin-11 and regulates oligodendrocyte development. *Am. J. Physiol. Cell Physiol.* **291**, C687–C698 (2006).
67. P. Bankhead *et al*., QuPath: Open source software for digital pathology image analysis. *Sci. Rep.* **7**, 16878 (2017).